*Supplementary Material for:*

# Vibrational and Thermodynamic Properties of Hydrous Iron-Bearing Lowermost Mantle Minerals

**Jiajun Jiang [1,2], Joshua M.R. Muir [2] and Feiwu Zhang [2,\*]**

[1]  Faculty of Land Resources Engineering, Kunming University of Science and Technology, Kunming 650093, China; jiangjiajun@ kust.edu.cn

[2]  State Key Laboratory of Ore Deposit Geochemistry, Institute of Geochemistry, Chinese Academy of Sciences, Guiyang 550081, China; j.m.r.muir@mail.gyig.ac.cn
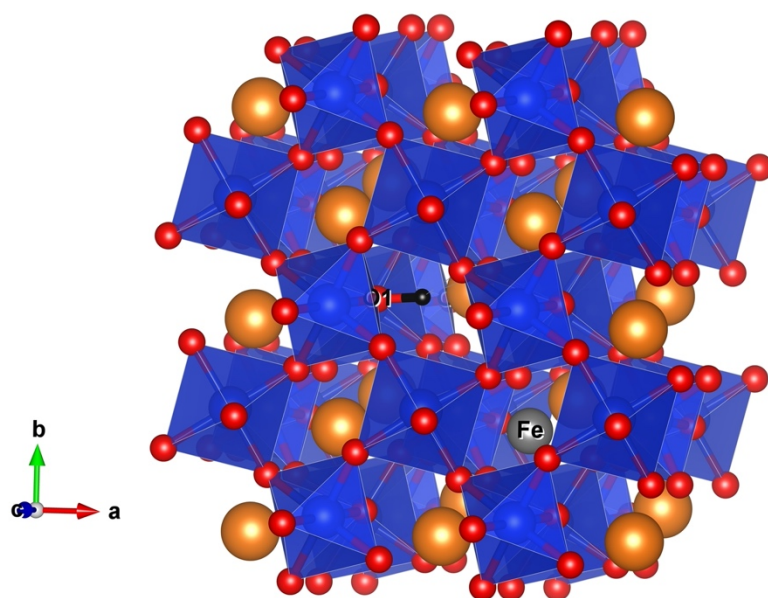
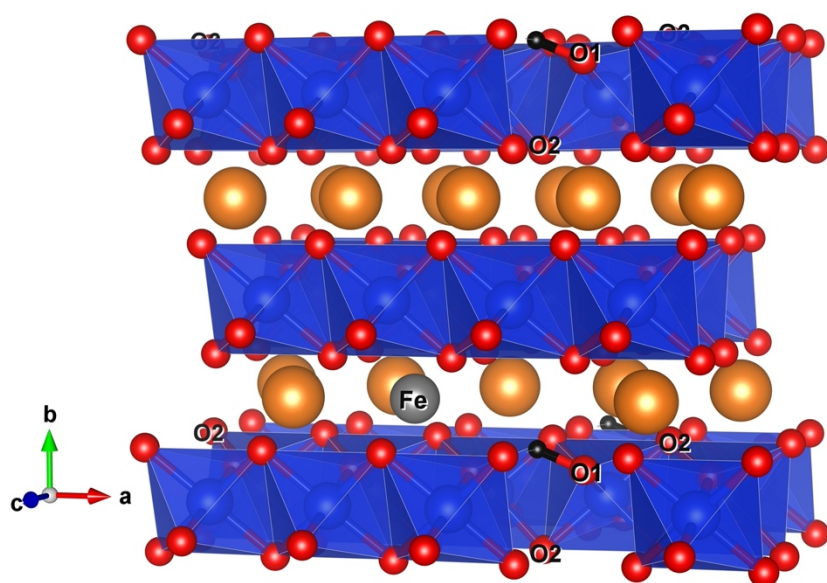\*  Correspondence: zhangfeiwu@vip.gyig.ac.cn
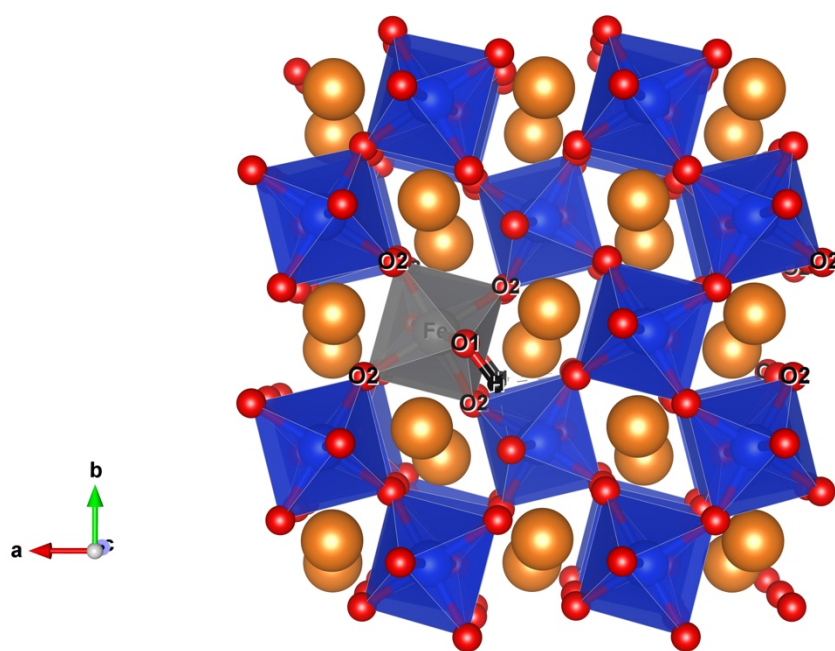
**Figure S1.** Crystal structures in details of $[Fe^{3+}-H]_{Si}$-Brg. In lattice structure, orange, dark blue, red, gray and black spheres represent magnesium, silicon, oxygen, iron and hydrogen, respectively.
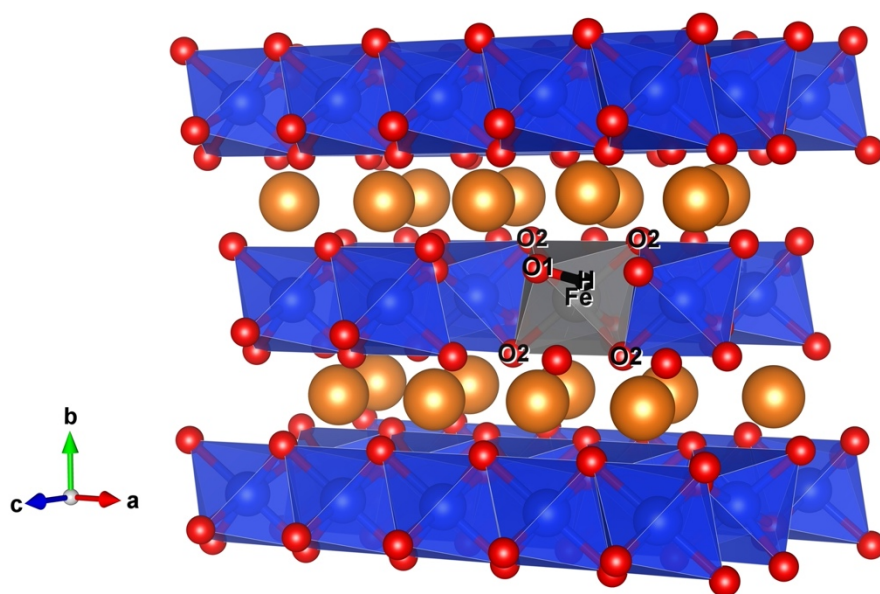
**Figure S2.** Crystal structures in details of $[Fe^{3+}-H]_{Si}$-PPv. In lattice structure, orange, dark blue, red, gray and black spheres represent magnesium, silicon, oxygen, iron and hydrogen, respectively.

**Figure S3.** Crystal structures in details of $[Fe^{3+}\text{-H}]_{\text{Mg-Mg}}$-Brg. In lattice structure, orange, dark blue, red, gray and black spheres represent magnesium, silicon, oxygen, iron and hydrogen, respectively.

**Figure S4.** Crystal structures in details of $[Fe^{3+}-H]_{Mg-Mg}$-PPv. In lattice structure, orange, dark blue, red, gray and black spheres represent magnesium, silicon, oxygen, iron and hydrogen, respectively.
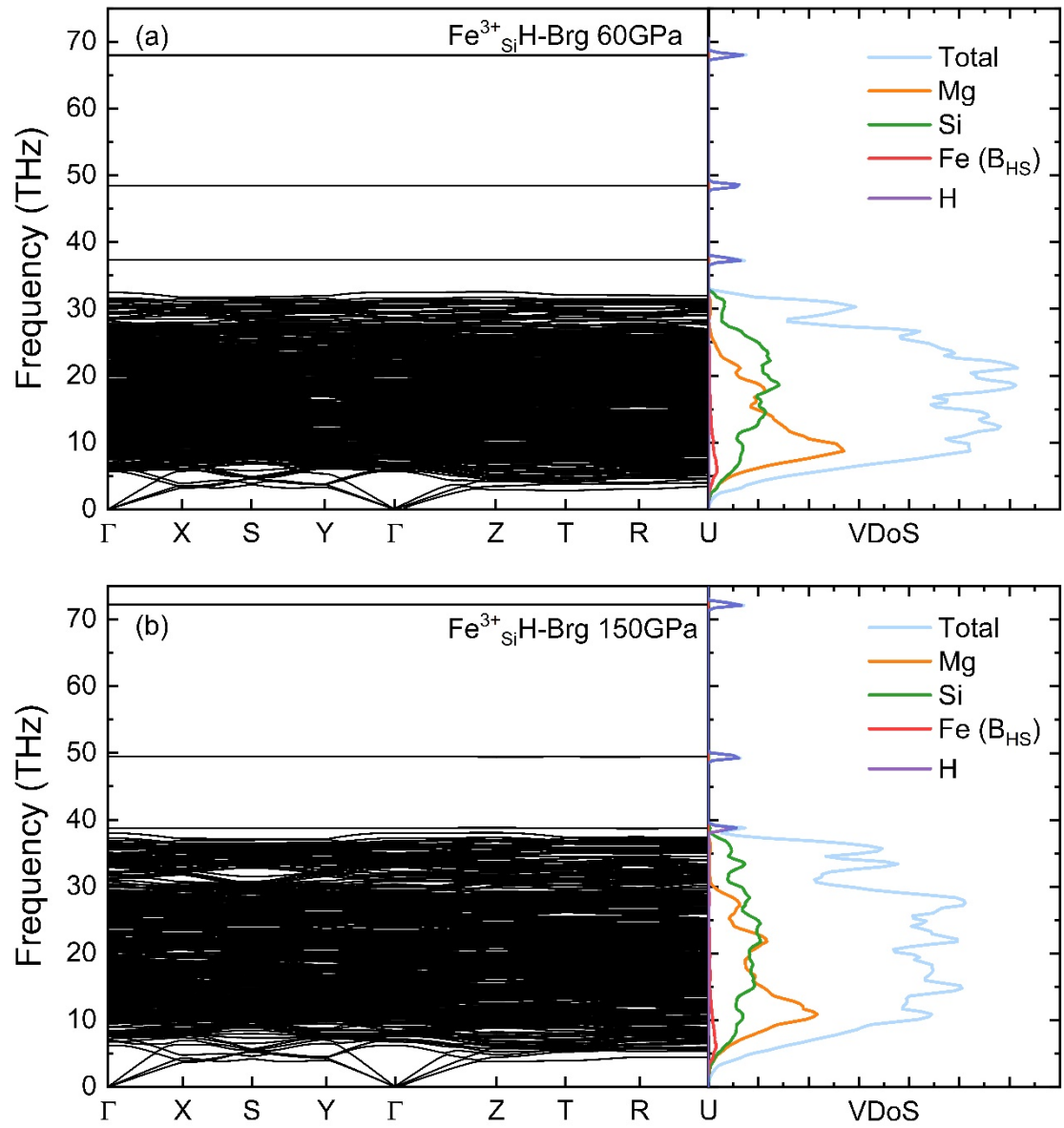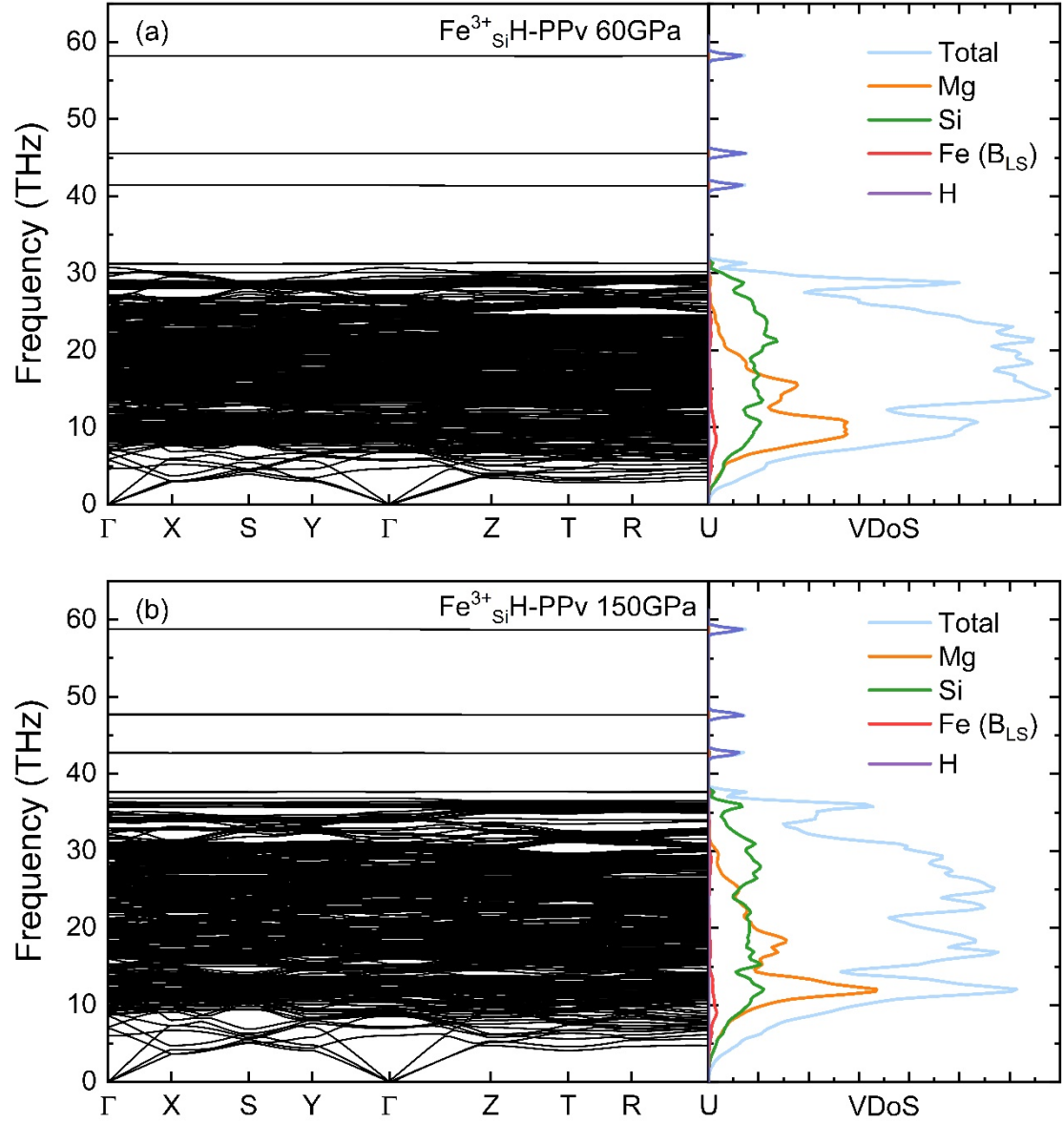
**Figure S5.** Phonon dispersion curves and vibrational density of states (VDoS) of [$Fe^{3+}$-H]$_{Si}$-Brg with HS $Fe^{3+}$ at 60 GPa (a) and 150 GPa (b). $B_{HS}$ indicates that the high spin $Fe^{3+}$ in B site (Si site). Total VDoS and partial VDoS of Mg, Si, Fe (HS), H are shown by light blue, orange, green, red and purple, respectively.

**Figure S6.** Phonon dispersion curves and vibrational density of states (VDoS) of [$Fe^{3+}$-H]$_{Si}$-PPv with LS $Fe^{3+}$ at 60 GPa (a) and 150 GPa (b). $B_{LS}$ indicates that the low spin $Fe^{3+}$ in B site (Si site). Total VDoS and partial VDoS of Mg, Si, Fe (LS), H are shown by light blue, orange, green, red and purple, respectively.
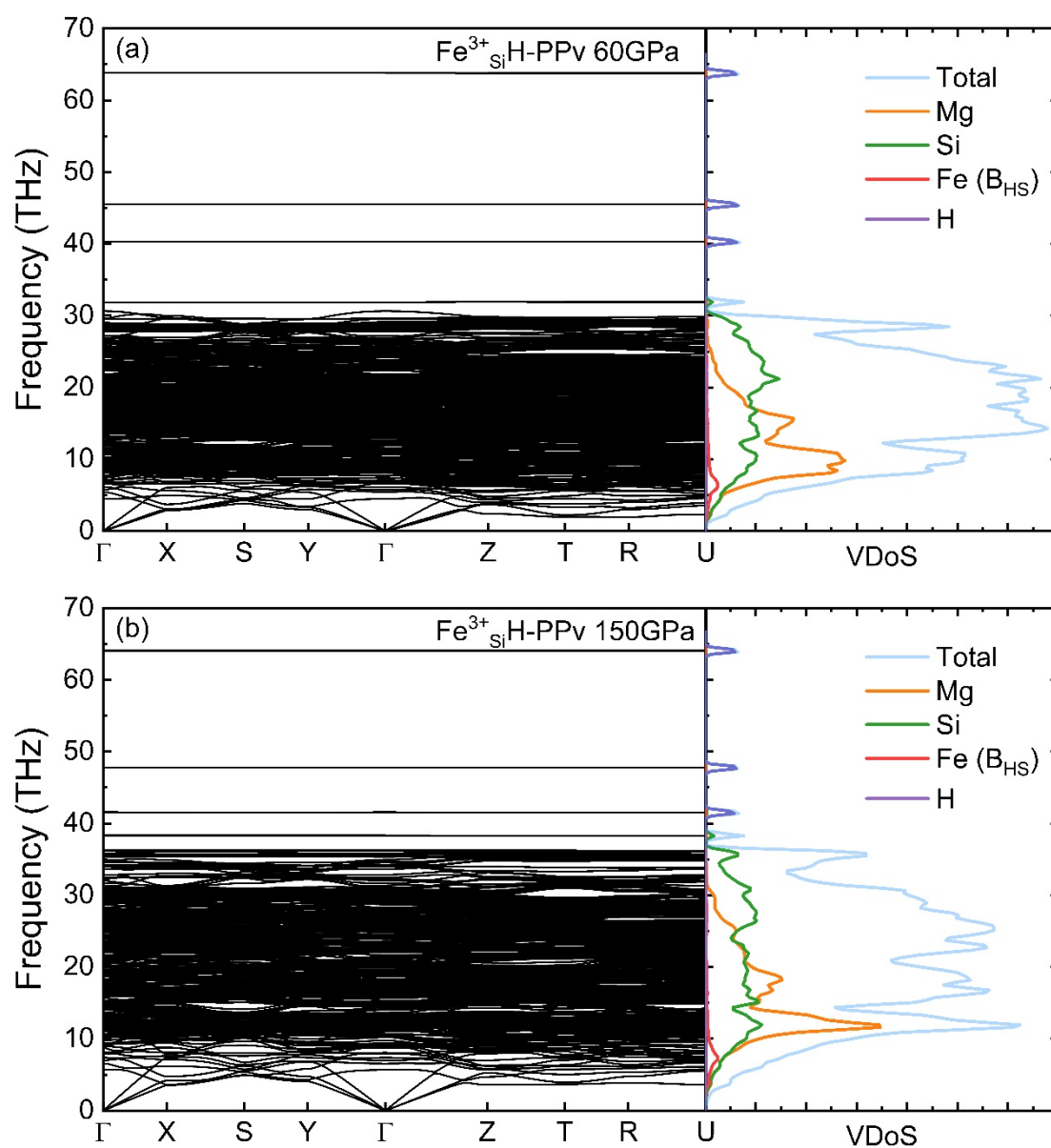
**Figure S7.** Phonon dispersion curves and vibrational density of states (VDoS) of [$Fe^{3+}$-H]$_{Si}$-PPv with HS $Fe^{3+}$ at 60 GPa (a) and 150 GPa (b). $B_{HS}$ indicates that the high spin $Fe^{3+}$ in B site (Si site). Total VDoS and partial VDoS of Mg, Si, Fe (HS), H are shown by light blue, orange, green, red and purple, respectively.

**Figure S8.** Phonon dispersion curves and vibrational density of states (VDoS) of $[Fe^{3+}-H]_{Mg-Mg}$-PPv at 60 GPa (a) and 150 GPa (b). $A_{HS}$ indicates that the high spin $Fe^{3+}$ in A site (Mg site). Total VDoS and partial VDoS of Mg, Si, Fe (HS), H are shown by light blue, orange, green, red and purple, respectively.
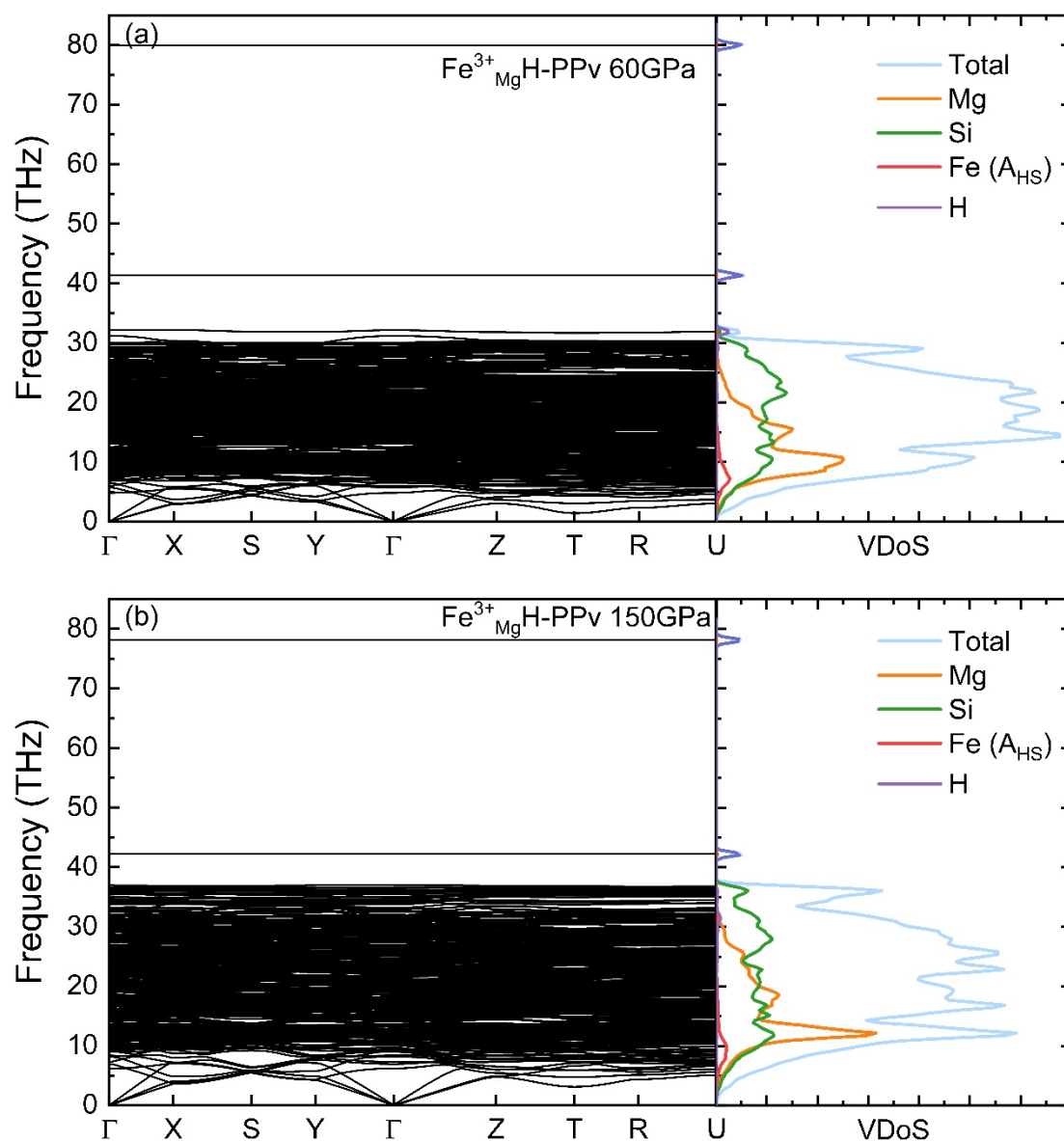
**Table S1.** Calculated thermodynamic parameters of hydrous iron-bearing and pure structure for bridgmanite*

| | 90 GPa | | | | 120 GPa | | | | 150 GPa | | | |
|---|---|---|---|---|---|---|---|---|---|---|---|---|
| | 300K | 1000K | 2000K | 3000K | 300K | 1000K | 2000K | 3000K | 300K | 1000K | 2000K | 3000K |
| $K_T$ (GPa) | 534.1 | 518.5 | 493.9 | 467.5 | 628.2 | 614.6 | 593.1 | 570.2 | 714.8 | 703.3 | 685.2 | 665.7 |
| | 536.9 | 520.6 | 495.1 | 468.4 | 632.1 | 617.8 | 595.1 | 571.2 | 719.8 | 707.7 | 688.1 | 667.3 |
| | 540.1 | 525.8 | 502.4 | 476.9 | 630.2 | 619.6 | 601.3 | 580.9 | 709.5 | 702.9 | 690.4 | 675.5 |
| $\alpha$ ($10^{-5}$ $K^{-1}$) | 0.74 | 1.38 | 1.53 | 1.63 | 0.60 | 1.17 | 1.29 | 1.35 | 0.51 | 1.04 | 1.14 | 1.18 |
| | 0.71 | 1.36 | 1.51 | 1.61 | 0.56 | 1.14 | 1.26 | 1.32 | 0.47 | 1.00 | 1.10 | 1.14 |
| | 0.69 | 1.34 | 1.48 | 1.57 | 0.58 | 1.16 | 1.26 | 1.31 | 0.53 | 1.07 | 1.15 | 1.17 |
| $C_P$ (J $mol^{-1}$ $K^{-1}$) | 64.4 | 118.9 | 128.7 | 133.1 | 60.2 | 117.4 | 127.4 | 131.3 | 56.7 | 116.1 | 126.5 | 130.2 |
| | 63.1 | 117.3 | 126.9 | 131.2 | 59.0 | 115.7 | 125.6 | 129.4 | 55.6 | 114.4 | 124.7 | 128.2 |
| | 63.3 | 117.7 | 127.0 | 131.1 | 59.1 | 116.2 | 125.9 | 129.5 | 55.6 | 115.0 | 125.2 | 128.7 |
| $\gamma$ | 1.23 | 1.25 | 1.26 | 1.28 | 1.18 | 1.20 | 1.21 | 1.22 | 1.15 | 1.18 | 1.18 | 1.18 |
| | 1.20 | 1.23 | 1.25 | 1.26 | 1.13 | 1.17 | 1.18 | 1.19 | 1.10 | 1.14 | 1.14 | 1.15 |
| | 1.17 | 1.23 | 1.25 | 1.26 | 1.17 | 1.20 | 1.21 | 1.21 | 1.23 | 1.21 | 1.20 | 1.20 |
| $S_{vib}$ (J $mol^{-1}$ $K^{-1}$) | 38.6 | 153.0 | 236.2 | 286.7 | 35.5 | 147.4 | 230.6 | 281.0 | 32.4 | 141.4 | 224.2 | 274.5 |
| | 38.2 | 151.6 | 234.2 | 284.0 | 34.5 | 144.8 | 226.9 | 276.7 | 31.7 | 139.1 | 220.9 | 270.5 |
| | 37.5 | 151.4 | 234.2 | 284.1 | 33.8 | 144.5 | 226.8 | 276.6 | 31.3 | 141.7 | 223.7 | 273.4 |

*Values in the first, second and third lines in each thermodynamic parameter are for $[Fe^{3+}-H]_{Si}$-Brg, $[Fe^{3+}-H]_{Mg-Mg}$-Brg and pure-Brg, respectively.

**Table S2.** Calculated thermodynamic parameters of hydrous iron-bearing and pure structure for post-perovskite*

| | 90 GPa | | | | 120 GPa | | | | 150 GPa | | | |
|---|---|---|---|---|---|---|---|---|---|---|---|---|
| | 300K | 1000K | 2000K | 3000K | 300K | 1000K | 2000K | 3000K | 300K | 1000K | 2000K | 3000K |
| $K_T$ (GPa) | 529.5 | 512.2 | 485.7 | 458.2 | 630.1 | 614.7 | 590.7 | 565.7 | 723.4 | 709.9 | 688.6 | 666.3 |
| | 527.9 | 511.0 | 485.1 | 458.5 | 632.8 | 617.4 | 593.4 | 568.7 | 731.9 | 718.0 | 696.3 | 673.6 |
| | 532.9 | 517.1 | 492.3 | 466.1 | 629.0 | 616.0 | 595.1 | 572.7 | 714.3 | 704.3 | 687.8 | 669.6 |
| $\alpha$ ($10^{-5}$ K$^{-1}$) | 0.76 | 1.42 | 1.58 | 1.68 | 0.59 | 1.18 | 1.31 | 1.38 | 0.49 | 1.03 | 1.14 | 1.18 |
| | 0.74 | 1.39 | 1.54 | 1.64 | 0.57 | 1.15 | 1.27 | 1.34 | 0.47 | 1.00 | 1.10 | 1.15 |
| | 0.72 | 1.38 | 1.53 | 1.62 | 0.58 | 1.17 | 1.28 | 1.34 | 0.51 | 1.05 | 1.15 | 1.18 |
| $C_P$ (J mol$^{-1}$ K$^{-1}$) | 63.7 | 119.2 | 128.7 | 133.4 | 59.4 | 117.6 | 127.5 | 131.4 | 55.8 | 116.3 | 126.6 | 130.2 |
| | 62.3 | 117.4 | 127.0 | 131.2 | 58.1 | 115.9 | 125.7 | 129.4 | 54.7 | 114.6 | 124.8 | 128.3 |
| | 62.6 | 117.9 | 127.1 | 131.3 | 58.2 | 116.4 | 125.9 | 129.6 | 54.7 | 115.1 | 125.2 | 128.7 |
| $\gamma$ | 1.24 | 1.25 | 1.26 | 1.28 | 1.17 | 1.19 | 1.20 | 1.21 | 1.13 | 1.16 | 1.17 | 1.17 |
| | 1.21 | 1.22 | 1.23 | 1.24 | 1.15 | 1.17 | 1.18 | 1.19 | 1.12 | 1.14 | 1.15 | 1.16 |
| | 1.19 | 1.23 | 1.24 | 1.26 | 1.15 | 1.19 | 1.20 | 1.20 | 1.17 | 1.18 | 1.18 | 1.18 |
| $S_{vib}$ (J mol$^{-1}$ K$^{-1}$) | 37.1 | 152.3 | 236.1 | 286.7 | 33.3 | 145.2 | 228.5 | 279.0 | 30.4 | 139.3 | 222.3 | 272.6 |
| | 36.2 | 149.5 | 232.2 | 282.0 | 32.5 | 142.6 | 224.9 | 274.6 | 29.7 | 137.0 | 218.8 | 268.5 |
| | 35.1 | 149.1 | 232.0 | 281.9 | 31.5 | 142.2 | 224.6 | 274.4 | 29.1 | 136.9 | 222.1 | 271.8 |

*Values in the first, second and third lines in each thermodynamic parameter are for [Fe$^{3+}$-H]$_{Si}$-PPv, [Fe$^{3+}$-H]$_{Mg-Mg}$-PPv and pure-PPv, respectively.
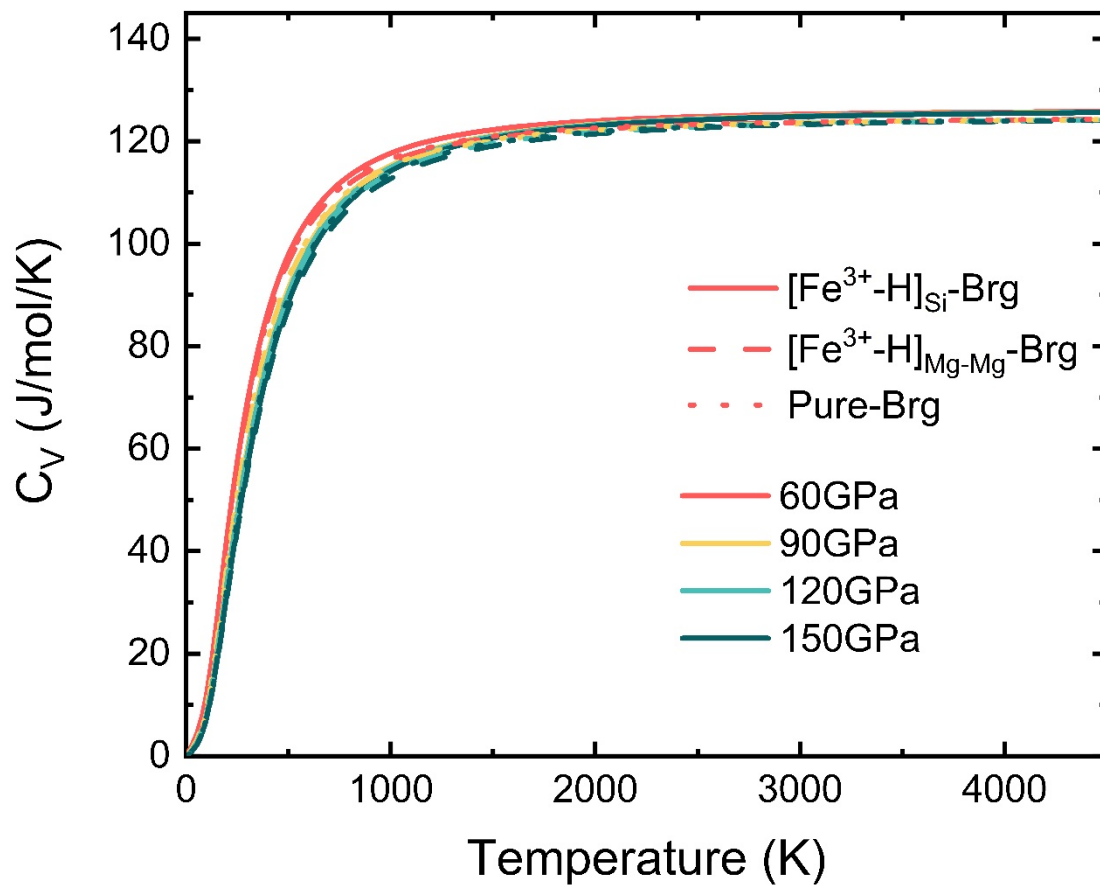
**Figure S9.** The heat capacity at constant volume as a function of temperature at different pressures. Solid, dashed and dotted lines represent the $[Fe^{3+}-H]_{Si}$-Brg, $[Fe^{3+}-H]_{Mg-Mg}$-Brg and Pure-Brg, respectively.
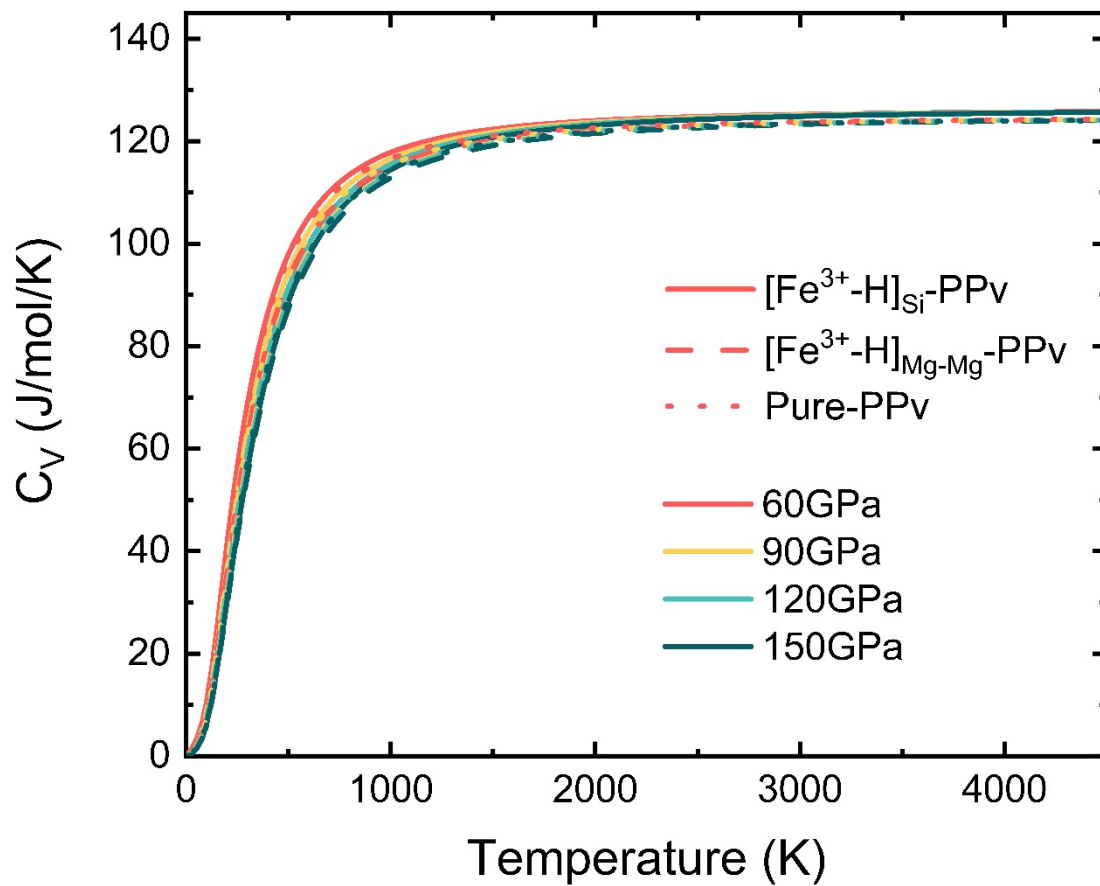
**Figure S10.** The heat capacity at constant volume as a function of temperature at different pressures. Solid, dashed and dotted lines represent the $[Fe^{3+}-H]_{Si}$-PPv, $[Fe^{3+}-H]_{Mg-Mg}$-PPv and Pure-PPv, respectively.
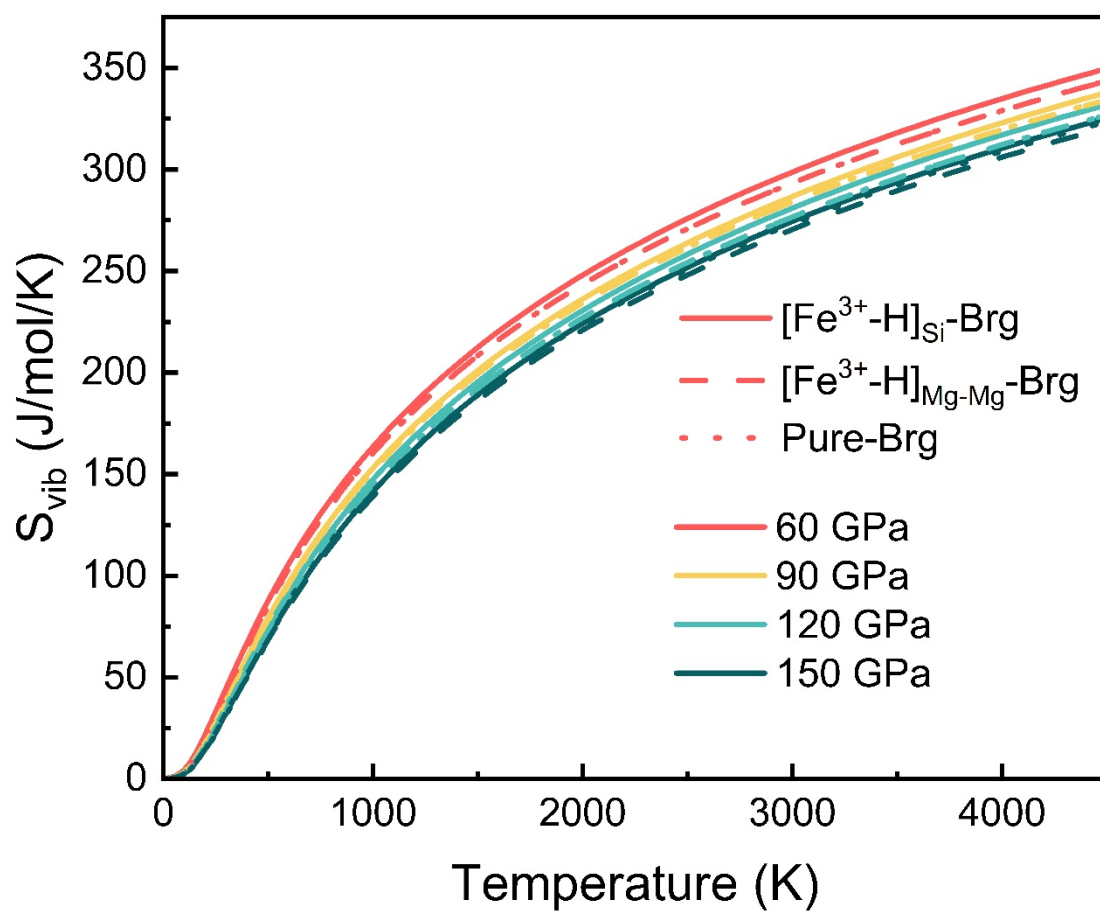
**Figure S11.** Temperature dependence of vibrational entropy at different pressures. Solid, dashed and dotted lines represent the $[Fe^{3+}\text{-H}]_{Si}$-Brg, $[Fe^{3+}\text{-H}]_{Mg\text{-}Mg}$-Brg and Pure-Brg, respectively.
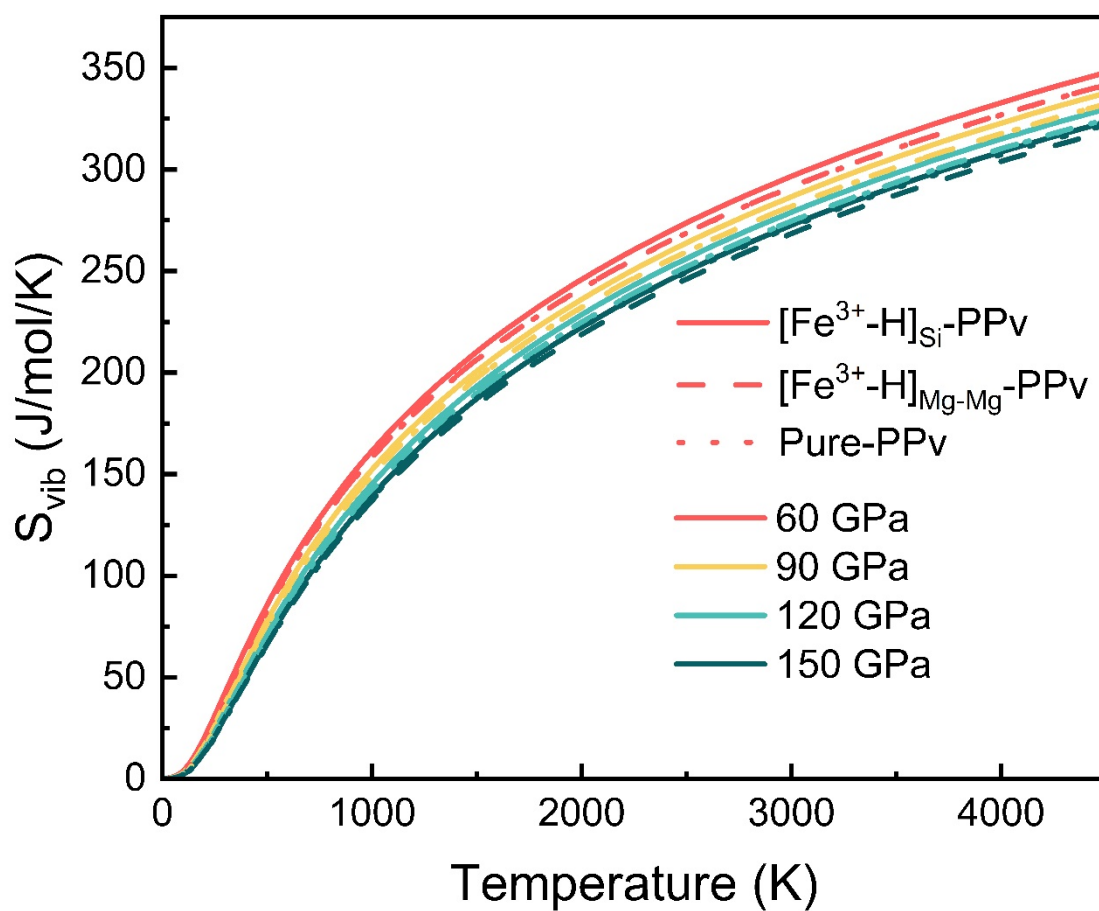
**Figure S12.** Temperature dependence of vibrational entropy at different pressures. Solid, dashed and dotted lines represent the $[Fe^{3+}-H]_{Si}$-PPv, $[Fe^{3+}-H]_{Mg-Mg}$-PPv and Pure-PPv, respectively.